



Get Clarity On Generics

Cost-Effective CT & MRI Contrast Agents



FRESENIUS
KABI

WATCH VIDEO

AJNR

Unruptured intracranial arteriovenous malformations do cause mass effect.

A J Kumar, F Viñuela, A J Fox and A E Rosenbaum

AJNR Am J Neuroradiol 1985, 6 (1) 29-32

<http://www.ajnr.org/content/6/1/29>

This information is current as
of August 11, 2025.

Unruptured Intracranial Arteriovenous Malformations Do Cause Mass Effect

Ashok J. Kumar¹
 Fernando Viñuela²
 Allan J. Fox²
 Arthur E. Rosenbaum¹

Sixty patients with clinically unruptured intracranial arteriovenous malformations were studied with high-resolution computed tomography. In 33, local and distant mass effects were evidenced by compression, distortion, and displacement of normal anatomic structures by the malformation, its afferent and efferent vessels, and the surrounding edema.

In the angiographic literature [1] in the pre-computed tomographic (CT) era, the demonstration of mass effect was taken as *prima facie* evidence that rupture had occurred within the demonstrated arteriovenous malformation (AVM). Mass effect, as shown by CT, occurred in a *high* percentage (55%) of our cases. Our study affirms that rupture is not a requirement for mass effects from AVMs and details the morphologic characteristics of large AVMs, which have substantial mass effect and cause displacement of adjacent structures in the absence of hemorrhage. Interrelated causes are discussed.

Subjects and Methods

Sixty patients with unusually large unruptured AVMs, proved by CT and angiography, were evaluated at the University Hospital, London, Ontario. These malformations were characterized by angiography and were judged to be pial in 59 and dural in one. A General Electric CT/T 8800 CT scanner was used, and preenhancement scans were obtained in all cases with intravenous enhancement accomplished by the bolus injection of 100 ml of concentrated contrast material (Conray 400, Mallinckrodt). Slice thickness was usually 10 mm with contiguous sections made without overlap for supratentorial lesions. For infratentorial detail, 5 mm sectioning was used. The angiographic and CT findings were reviewed prospectively by two authors (F. V. and A. J. F.) and retrospectively by the other two authors (A. J. K. and A. E. R.).

The presenting signs and symptoms in the 24 supratentorial AVMs that had mass effect were varied: 12 were seen with headache (including two with migraine), 14 had seizures, and two had progressive weakness of the extremities. Two patients were referred for potential embolization of a frontal AVM; one had hemorrhaged 4 years and the other 3 months earlier. Three patients had subarachnoid hemorrhage on lumbar puncture on previous admissions 2 years, 2 months, and 1 week before the current study. Of the nine posterior fossa AVMs producing mass effect, two were seen with tic douloureux and one with headache. Two other patients were admitted for possible embolization of pontine AVMs that had hemorrhaged 4 and 3 years earlier. The last four (of nine) patients had subarachnoid hemorrhage, and one had a coexisting middle cerebral artery aneurysm that had ruptured. No patient had clinical evidence of rupture of AVM with intraaxial hematoma.

Four CT criteria were used to rule out hematoma as the cause of mass effect from the AVM: (1) the precontrast scan showed no hyperdensity beyond that ascribed to blood (confirmed by enhancement) within either the blood vessel or the malformation; (2) the CT scan was correlated with the angiogram to assure close correspondence of vessels; (3) after intravenous enhancement, no areas of enhancement were attributable to extravasation (e.g., as seen in contusion or opacifying epidural hematoma); and (4) the ultimate criterion was that

Received May 5, 1983; accepted after revision July 5, 1984.

¹ Russell H. Morgan Department of Radiology and Radiological Sciences, Johns Hopkins Medical Institutions, Baltimore, MD 21205. Address reprint requests to A. J. Kumar, Neuroradiology Section.

² Departments of Diagnostic Radiology and Clinical Neurological Sciences, University Hospital, University of Western Ontario, London, Ontario, Canada N6A 5A5.

AJNR 6:29-32, January/February 1985
 0195-6108/85/0601-0029 \$00.00
 © American Roentgen Ray Society

TABLE 1: Structures Affected by AVMs Producing Mass Effect

Location of AVM: Effect	No. of Cases
Supratentorial:	
Lateral ventricles compressed (only)	5
Lateral ventricles displaced	12
Third ventricle displaced	9
Pineal gland displaced	14
Choroid plexus displaced	8
Cortical sulci obliterated	10
Inner table of skull eroded	3
Parasellar cistern compressed	1
Infratentorial:	
Fourth ventricle compressed	4
Fourth ventricle displaced	5

Note.—AVM = arteriovenous malformation.

TABLE 2: Factors Contributing to Mass Effect in AVMs

Factor	No. by Location	
	Supratentorial	Infratentorial
Size of AVM:		
3–5 cm	19	6
1–3 cm	5	3
Venous sacs/ectatic veins	11	3
White-matter edema	2	0

Note.—AVM = arteriovenous malformation.

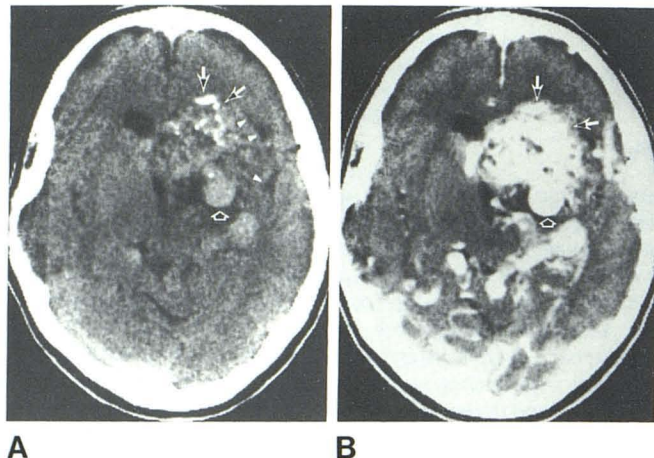


Fig. 1.—Before (A) and after (B) enhancement. Large partly calcified deep frontal AVM (long arrows). Mass effect by AVM manifested by compression of regional ventricular system and lateral displacement of medial part of sylvian fissure (arrowheads). Dilated venous sac (short arrow) contributes to mass effect regionally and distally.

the aggregation of afferent vessels, AVM nidus, efferent vessels, and surrounding edema was proportional to the mass effect.

Results

A multiplicity of factors contributed to or produced mass effect. Structures affected in the 24 examples of supratentorial AVMs (occipital lobe, nine; frontal lobe, eight; parietal lobe,

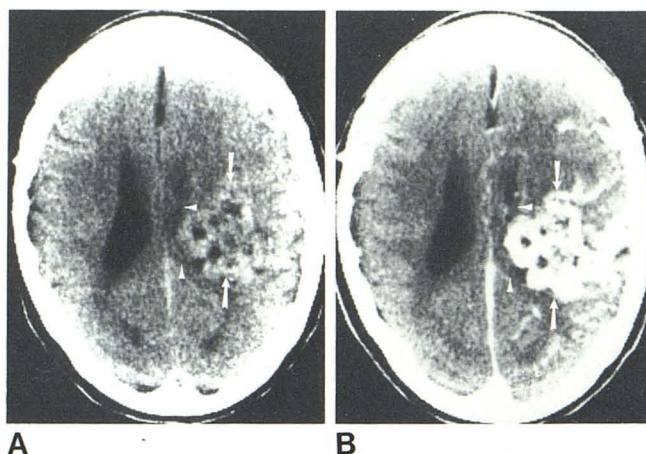


Fig. 2.—Before (A) and after (B) enhancement. Large parietal AVM (arrows) before (A) and after (B) enhancement produces compression and distortion of ipsilateral ventricle (arrowheads) and surround.

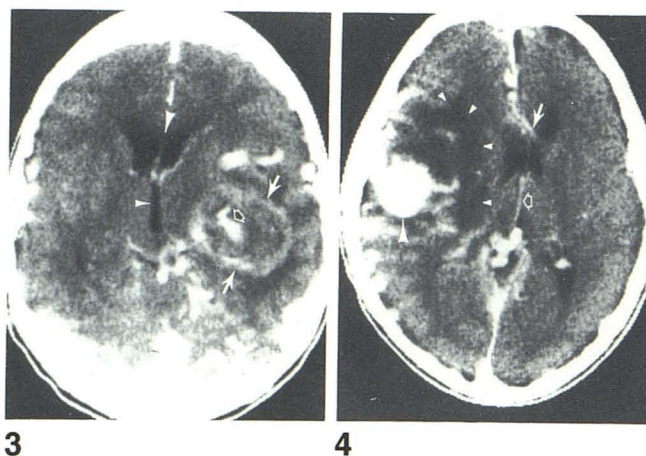


Fig. 3.—After enhancement. Large dilated varix (solid arrows) (proven angiographically) produces shift of third ventricle (small arrowhead), ipsilateral frontal horn, and septum pellucidum (large arrowhead). Opacified lumen within partly thrombosed varix (open arrow).

Fig. 4.—After enhancement. Edema of white matter (small arrowheads) accompanies high parietal AVM (nidus not shown) responsible for displacement of anterior cerebral artery (solid arrow), frontal horn, septum pellucidum, and internal cerebral vein (open arrow). Posterior aspect of large varix (large arrowhead).

six; temporal lobe, five; basal ganglia and thalamus, three; and more than one lobe involved, seven) and nine examples of infratentorial AVMs (cerebellar hemisphere, four; vermis, three; and pons, two) are summarized in table 1. Since clinically unruptured malformations are the subject of description, the size of the malformation that resulted in mass effect was cataloged as was the presence of venous ectasia and edema. The results of these observations are listed in table 2. Of the 33 AVMs, 25 were 3–5 cm in maximum diameter and eight were 1–3 cm. Of the 24 supratentorial AVMs that did not produce mass effect, only one was 3–5 cm, 20 were 1–3 cm, and three were less than 1 cm. In two cases of

Fig. 5.—After enhancement. Large dilated vein (*long arrow*) of occipital AVM, which causes anterior displacement of choroid plexus of lateral ventricle (*short arrow*).

Fig. 6.—After enhancement. Cerebellar AVM (*arrow*) causes rotary displacement of fourth ventricle (*arrowhead*).

Fig. 7.—After enhancement. Large AVM (*arrows*) occupies almost entire confines of cerebellar hemisphere while causing disproportionately small, forward displacement of fourth ventricle (*arrowhead*).

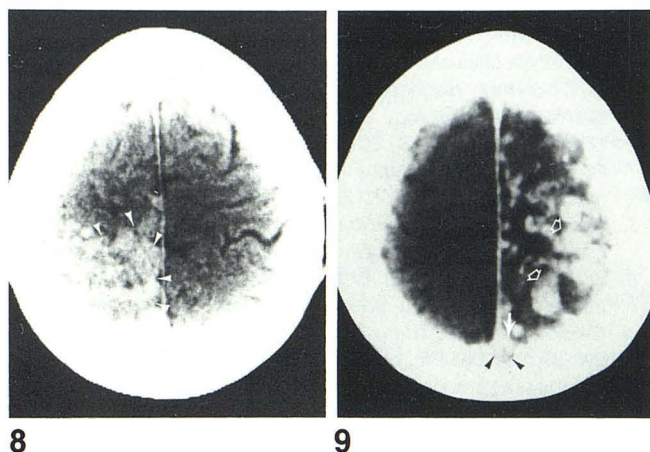
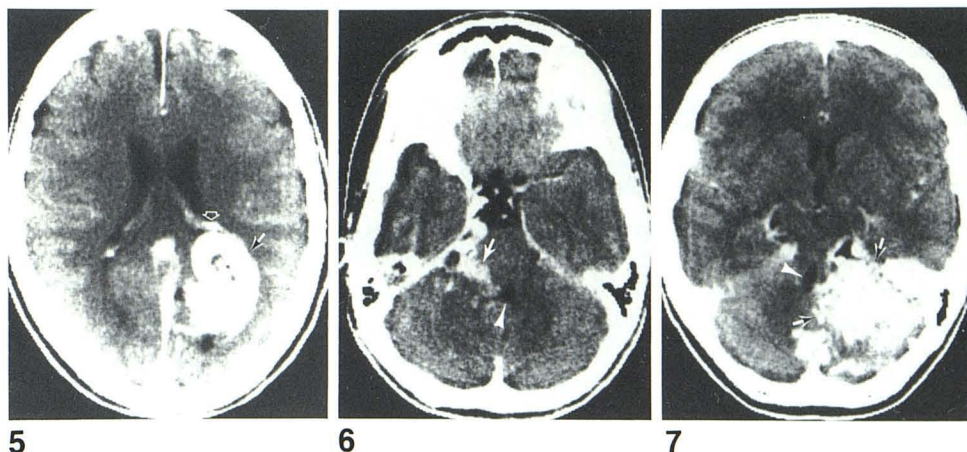


Fig. 8.—Before enhancement. Obliteration of normal corticomedullary interfaces and obscuration of cerebral sulci caused by high-convexity AVM (*arrowheads*).

Fig. 9.—After enhancement. Erosion of inner table of skull (*arrowheads*) near midline caused by enlarged superior sagittal sinus (*solid arrow*); exaggerated venous drainage into superior sagittal sinus is via large-convexity veins (*open arrows*).

supratentorial AVMs, gross displacement was related to the surrounding white-matter edema. Large dilated venous sacs were the cause of mass effect in 11 supratentorial AVMs and three infratentorial AVMs.

The features identified as mass effect in large intracranial AVMs are illustrated in figures 1–9: (1) displacement of supratentorial midline structures such as the septum pellucidum and third ventricle (figs. 1 and 3) and pineal gland; (2) compression and displacement of parts of the lateral ventricle(s) (figs. 1–4); (3) displacement of the choroid plexus in compressed or collapsed lateral ventricles (fig. 5); (4) compression and/or displacement of the fourth ventricle (figs. 6 and 7); (5) obliteration of cortical sulci (fig. 8); (6) erosion of the inner table of the skull (fig. 9); (7) compression and asymmetry of a cistern; (8) gross displacement related to surrounding edema (fig. 4); and (9) large dilated venous sacs (figs. 1, 3–5, and 9).

Discussion

Mass effect in unruptured AVMs has been illustrated or alluded to in the literature only since CT has been available [2–13]. Most articles, however, have dealt with the broad aspects of these lesions and have not delineated the morphologic characteristics of AVMs or the factors contributing to mass effect. CT has opened new avenues for imaging the details of these vascular lesions, showing the relation between the AVM, mass effects it produces on regional and distant structures, and concomitant acute hemorrhage. In the past, expansive or space-occupying features of AVMs implied hemorrhage, but in our cases, no instance of recent hemorrhage into brain substance or subdural or epidural spaces was suspected clinically or found by CT.

Previous authors have observed and discussed some manifestations of expansion from AVMs. Hayward [4] found significant ventricular distortion from the angioma in six cases. Kendall and Claveria [5] noted that while most angiomas did not exert significant mass effect relative to their extent, large ones did in 8.8% of cases. Terbrugge et al. [6] found that mass effect was present in 12 of their 22 cases, and Weisberg [7] noted mass effect in two cases. Britt et al. [8] found an encapsulated cystic choroid plexus AVM that simulated a colloid cyst of the third ventricle and presented as a mass. Even in angiographically occult AVMs of the brain, Bell et al. [9] observed mass effect on CT in three of six cases; Becker et al. [10] confirmed this in seven of their 15 cases. Purely dural malformations producing mass effect were observed by Miyasaka et al. [11] in *each* of their three cases. The presence of high-resolution CT scanning allows for precise determination of those morphologic structures and potential concomitants (e.g., edema) that produce mass effect in the absence of hematoma. We analyzed the factors that produced and/or contributed to the mass effect in our patients with intracranial AVMs:

Size

Mass effect largely correlated with the size of the AVM and its propinquity to discernible structures distorted by mass

effect (e.g., sulci, ventricles, cisterns, and pineal gland). The smallest AVM causing mass effect was 1 cm and the largest, 5 cm.

Ectasia of Large Arteries, Veins, and Varices

Distension of vessels of the AVM affected the subarachnoid spaces (predominantly basally) and the brain intrinsically. Regional distortion related to the size of the vessels of the AVM, their tortuosity, and the pathway they traversed. Veins, however, played a much larger role in producing mass effect than did arteries.

Edema

Edema from AVMs has been recognized [4, 5, 10–13], but massive edema has not been reported. Hayward [4] noted that cerebral tissue immediately adjacent to the angioma was hypodense in one of his 12 unruptured AVMs. Leblanc et al. [12] observed edema surrounding the AVM in one of five cases, and Kendall and Claveria [5] observed it once. Edema was also noted in occult malformations by Becker et al. [10] in five of 15 cases. Miyasaka et al. [11] demonstrated hypodensity of the white matter in two dural AVMs. In one of these two cases, the hypodensity of the brain returned to normal after embolization of the AVM. "This response suggests that the decreased CT density resulted mainly from the arteriovenous shunt and was not due solely to sinus occlusion" [11]. Conversely, in a dural AVM reported by Chiras et al. [13], edema of the temporal lobe caused contralateral shift of the lateral ventricle and was attributed to bilateral transverse sinus occlusion with rerouting of blood into the temporal, basilar, and sylvian veins. What was striking in our cases, however, is that the edema (hypodensity) could be very sizable and occupy an area larger than that of the opacified malformation. Diffuse white-matter hypodensity from edema as seen in two of our cases may be ascribed to vasogenic [14, 15] or ischemic origins.

In summary, mass effect was observed in 33 large, unruptured supra- and infratentorial AVMs, and the magnitude of mass effect largely paralleled the size of the AVM. Enlarged and/or tortuous veins, varices, and venous sacs contributed largely to the mass effect in 14 AVMs, while edema was the predominant component of mass effect in two AVMs.

ACKNOWLEDGMENTS

We thank C. E. Drake and colleagues for referring these patients to us, for the high clinical acumen manifested here by the care given these patients, and for the records they shared; we also thank Betty Brandt and Marge Eddy for assistance in manuscript preparation.

REFERENCES

1. Davidoff LM, Jacobson HG, Zimmerman HM. Vascular anomalies. In: *Neuroradiology workshop*, vol 3. *Nonneoplastic intracranial lesions*. New York: Grune & Stratton, 1968:298–357
2. Pressman BD, Kirkwood JR, David DO. Computerized transverse tomography of vascular lesions of the brain. Part 1: arteriovenous malformations. *AJR* 1975;124:208–214
3. Lukin RR, Chambers AA, Tomsick TA. Cerebral vascular lesions: infarction, hemorrhage, aneurysm and arteriovenous malformation. *Semin Roentgenol* 1977;12:77–89
4. Hayward RD. Intracranial arteriovenous malformations. Observations after experience with computerized tomography. *J Neurol Neurosurg Psychiatry* 1976;39:1027–1033
5. Kendall BE, Claveria LE. The use of computed axial tomography (CAT) for the diagnosis and management of intracranial angiomas. *Neuroradiology* 1976;12:141–160
6. Terbrugge K, Scotti G, Ethier R, Melançon D, Tchang S, Milner C. Computed tomography in intracranial arteriovenous malformations. *Radiology* 1977;122:703–705
7. Weisberg LA. Computed tomography in the diagnosis of intracranial vascular malformations. *Comput Radiol* 1979;3:125–132
8. Britt RH, Silverberg GD, Enzmann DR, Hanbery JW. Third ventricular choroid plexus arteriovenous malformation simulating a colloid cyst. *J Neurosurg* 1980;52:246–250
9. Bell BA, Kendall BE, Symon L. Angiographically occult arteriovenous malformations of the brain. *J Neurol Neurosurg Psychiatry* 1978;41:1057–1064
10. Becker DH, Townsend JJ, Kramer RA, Newton TH. Occult cerebrovascular malformations, a series of 18 histologically verified cases with negative angiography. *Brain* 1979;102:249–287
11. Miyasaka K, Takei H, Nomura M, et al. Computerized tomography findings in dural arteriovenous malformations. *J Neurosurg* 1980;53:698–702
12. Leblanc R, Ethier R, Little JR. Computerized tomography findings in arteriovenous malformations of the brain. *J Neurosurg* 1979;51:765–772
13. Chiras J, Bories J, Leger JM, Gaston A, Launay M. CT scan of dural arteriovenous fistulas. *Neuroradiology* 1982;23:185–194
14. Katzman R, Clasen R, Klatzo I, Meyer JS, Pappius HM, Waltz AG. Brain edema in stroke. Study group on brain edema in stroke. *Stroke* 1977;8:510–540
15. Drayer BP, Rosenbaum AE. Brain edema defined by computed tomography. *J Comput Assist Tomogr* 1979;3:327–333